A METHODOLOGY FOR GLOBAL SENSITIVITY ANALYSIS OF TRANSIENT CODE OUTPUT APPLIED TO A REFLOOD EXPERIMENT MODEL USING TRACE

Damar Wicaksono[1,2,*], **Omar Zerkak**[2], **and Andreas Pautz**[1,2]
Laboratory for Reactor Physics and Systems Behaviour (LRS)
[1]Ecole polytechnique fédérale de Lausanne, CH-1015 Lausanne, Switzerland
[2]Paul Scherrer Institut, CH-5232 Villigen-PSI, Switzerland
damar.wicaksono@epfl.ch; omar.zerkak@psi.ch; andreas.pautz@epfl.ch

ABSTRACT

Understanding properly the impact of model parameters and their interactions on the predictions is required for an appropriate model assessment. For simulation of reflooding following a LOCA, this requirement is justified because the important parameters affecting predictions often cannot be measured and should be considered uncertain. Moreover, different process representations in the model may have strong influence at different times of the transient. These issues complicate the task of model assessment.

In this work, a global sensitivity analysis (GSA) methodology tailored to analyze transient code output is developed. The methodology was based on the Morris and the Sobol' methods. The first was utilized to screen out non-influential parameters which allowed generation of larger samples with fewer code runs for the second method, the Sobol' method. The method results in global sensitivity indices quantifying the contribution of inputs variations to the output variation, considering interactions among them. The Functional Data Analysis (FDA) techniques were then used to post-process the output deriving new quantities of interest (QoI)s describing the overall functional variation.

The method was successfully applied to a reflood simulation model using the thermal-hydraulics (TH) system code TRACE with 26 input parameters. Complementing the conventional QoIs (such as the max. temperature and time of quenching), the FDA-derived quantities gave a deeper insight on particular modes of functional variation and attributing them to the variations of the model parameters. The temperature transient was divided into two modes: the ramp phase and the descent phase. The ramp phase showed that the model was additive in terms of the parameter variations with Dispersed Film Flow Boiling-related parameters explained most of the functional output variation. Yet, the variation during the descent could only be explained through parameters interactions. This indicated the non-identifiability of the model for that specific phase of the transient with respect to the temperature response.

KEYWORDS
PWR Reflood, Global Sensitivity Analysis, Functional Data Analysis, Morris Method, Sobol' Method

1. INTRODUCTION

This paper deals with global sensitivity analysis (GSA) of code output which is time-dependent. A goal of GSA is to apportion the variations in relevant output (quantity of interest, or QoI) according to the overall input variations taking into account interactions between the inputs. Typically, the QoI for GSA is a scalar produced by predefined scalar function (the maximum, the minimum, the average, etc.). In the context of

* Corresponding author

the analysis of the safety of nuclear thermal-hydraulic systems, the maximum cladding temperature is a usual example of a scalar function. But, there is also a need to analyze the transient output as a whole, beyond the conventional pre-defined scalar output (the max., min., average, etc.) as this might reveal extra features of the model behavior that were previously overlooked.

A sensitivity analysis methodology applicable to time-dependent simulations and based on two GSA methods is proposed in Section 2. Section 3 describes the chosen test case, a simulation of a FEBA reflood experiment using the TH system code TRACE and assuming 26 model parameters. The main results of the analysis are presented in Section 4, where various QoIs are considered, typical scalar values and values based on FDA techniques, to reveal salient features in the transient code output.

2. METHODOLOGY

2.1. Derivative-based Sensitivity Measure: the Morris Method

The key idea behind the Morris method [1] is to evaluate a local sensitivity measure called the *elementary effect* over the space of input parameters. From its statistics, the importance (or lack of it) of the input parameters can be inferred. By evaluating the elementary effect at randomly selected points in the input parameters space, the method takes into account nonlinearity and parameters interactions.

Consider a k-parameter model, where $\vec{X} = (x_1, \dots, x_k)$ is the vector of parameters and $Y = f(\vec{X})$ is the output of the model evaluated at point $\vec{X}$. The elementary effect of i-th parameter X_i is defined as,

$$EE_i = \frac{f(x_1,x_2,\dots,x_{i-1},x_i+\Delta,\dots,x_k)-f(x_1,x_2,\dots,x_{i-1},x_i,\dots,x_k)}{\Delta}; \quad \frac{1}{p-1} \le \Delta \le 1-\frac{1}{p-1} \tag{1}$$

Where Δ, the grid jump, is chosen such that $\vec{X} + \Delta$ is still in the domain of the parameters space; p is the number of levels that partitions the model parameters space into a uniform grid of points where the model is evaluated. The gridded space constructs a finite distribution of size of $p^{k-1}[p - \Delta(p-1)]$ of the elementary effects corresponding to each input parameter.

Supposed that a number n_r of EE_ihave been sampled from its finite distribution, the statistical summary of EE_i along the sampled trajectory can be calculated. The statistics include the mean, the standard deviation, and the mean of absolute values of the EE_i,

$$\mu_i = \frac{1}{n_r}\sum_{j=1}^{n_r} EE_i^j \; ; \qquad \sigma_i = \sqrt{\frac{1}{n_r}\sum_{j=1}^{n_r}\left(EE_i^j - \mu_i\right)^2} \; ; \qquad \mu_i^* = \frac{1}{n_r}\sum_{j=1}^{n_r} |EE_i^j| \; ; \tag{2}$$

where EE_i^j is the elementary effect of the parameter i on the j-th point of the sampled trajectories. The mean gives the global influence of the i-th parameter on the output Y, while the standard deviation gives indication of the presence of nonlinearity or parameters interactions. To avoid any cancellation effect when evaluating the mean, [2] proposed the third statistics using absolute value.

The statistics of EE_i provide a measure of global sensitivity on the importance of parameter X_i. First, if μ_i (or μ_i^*) and σ_i both are small then parameter X_i is deemed non-influential. Second, if μ_i (or μ_i^*) is large but σ_i is small then parameter X_i is considered as influential with linear effect. Third, a large value of σ_i indicates nonlinearities or interactions of parameter X_i with other parameters.

2.2. Variance-based Sensitivity Measure: the Sobol'-Saltelli Method

Variance-based methods decompose the output variance into contributions of the input variances. Consider a mathematical model $Y = f(\vec{X})$ giving a scalar output for a given set of k-dimensional inputs parameters $\vec{X}$. A high-dimensional model representation (HDMR) [3] of $f(\vec{X})$ is a linear combination of functions with increasing dimensionality (up to k-dimension),

$$f(\vec{X}) = f_o + \sum_{i=1}^{k} f_i(x_i) + \sum_{1\le i<j<k} f_{ij}(x_i, x_j) + \cdots + f_{12..k}\,(x_1, x_2, \ldots x_k) \tag{3}$$

Representation in Eq. (3) is not unique, but a special unicity condition (see [4] for details)

$$\int f_{i1,i2,\ldots is}(x_{i1}, \ldots, x_{is})\, dx_m = 0 \text{ for } m = i_1, i_2, \ldots, i_s\ , s \in \{1, .. k\} \tag{4}$$

gives the orthogonality property to the functions as well as uniqueness to the representation. Consider now that the input vector $\vec{\boldsymbol{X}}$ contains k independent random variables $\{X_i, i = 1,2, \ldots k\}$ with the uniform distribution over the unit hypercube $\{\Omega = \vec{\boldsymbol{X}} | 0 \le x_i \le 1; i = 1,2, \ldots k\}$. Using Eq. (3)-(4) it follows that

$$\begin{gathered} f_o = \mathbb{E}[\boldsymbol{Y}]; \\ f_i(\boldsymbol{X_i}) = \mathbb{E}_{\sim i}[\boldsymbol{Y}|\boldsymbol{X_i}] - \mathbb{E}[\boldsymbol{Y}]; \\ f_{ij}(\boldsymbol{X_i}, \boldsymbol{X_j}) = \mathbb{E}_{\sim ij}[\boldsymbol{Y}|\boldsymbol{X_i}, \boldsymbol{X_j}] - \mathbb{E}_{\sim i}[\boldsymbol{Y}|\boldsymbol{X_i}] - \mathbb{E}_{\sim j}[\boldsymbol{Y}|\boldsymbol{X_j}] - \mathbb{E}[\boldsymbol{Y}] \end{gathered} \tag{5}$$

And the same follows for higher-order terms. In the above, $\mathbb{E}[\cdot \mid \cdot]$ means the conditional expectation and $\sim i$ in the subscript means integration over all parameter but i. Applying the variance operator on $\boldsymbol{Y}$,

$$\mathbb{V}[\boldsymbol{Y}] = \sum_{i=1}^{k} \mathbb{V}[f_i(\boldsymbol{X_i})] + \sum_{1\le i<j<k} \mathbb{V}[f_i(\boldsymbol{X_i}, \boldsymbol{X_j})] + \cdots + \mathbb{V}[f_{12..k}(\boldsymbol{X_1}, \boldsymbol{X_2}, \ldots \boldsymbol{X_k})] \tag{6}$$

Which is termed the ANOVA-HDMR ([4], [5]): the variance of the output is decomposed into summands of the first- and higher-order effects of the input variances. Division by $\mathbb{V}[\boldsymbol{Y}]$ aptly normalizes Eq. (6),

$$1 = \sum_{i=1}^{k} S_i + \sum_{1\le i<j<k} S_{ij} + \cdots + S_{12\ldots k} \tag{7}$$

The Sobol' main-effect sensitivity index of parameter X_i is then defined as,

$$S_i \equiv \frac{\mathbb{V}_i[\mathbb{E}_{\sim i}[\boldsymbol{Y}|\boldsymbol{X_i}]]}{\mathbb{V}[\boldsymbol{Y}]} \tag{8}$$

The nominator is the variance of the conditional expectation and the index is a global sensitivity measure interpreted as the amount of variance reduction in the model output if the variation of X_i is fixed.

A related sensitivity index proposed in [6] is the total-effect sensitivity index defined as

$$ST_i \equiv \frac{\mathbb{E}_{\sim i}[\mathbb{V}_i[\boldsymbol{Y}|\boldsymbol{X}_{\sim i}]]}{\mathbb{V}[\boldsymbol{Y}]} = \frac{1 - \mathbb{V}_{\sim i}[\mathbb{E}_i[\boldsymbol{Y}|\boldsymbol{X}_{\sim i}]]}{\mathbb{V}[\boldsymbol{Y}]} \tag{9}$$

This index, a global measure, is interpreted as the amount of variance left in the output if the variations of all input parameters but the i-th could be fixed. The difference between Eq. (8) and Eq. (9) quantifies the amount of interaction parameter X_i has.

To compute the sensitivity index defined above, the variance and expectation operators are written in their integral form. First, the variance operator shown in the nominator of Eq. (8) is rewritten as,

$$\mathbb{V}_i\left[\mathbb{E}_{\sim i}[\boldsymbol{Y}|\boldsymbol{X_i}]\right] = \mathbb{E}_i[\mathbb{E}^2_{\sim i}[\boldsymbol{Y}|\boldsymbol{X_i}]] - \left(\mathbb{E}_i\left[\mathbb{E}_{\sim i}[\boldsymbol{Y}|\boldsymbol{X_i}]\right]\right)^2 = \int \mathbb{E}^2_{\sim i}\,[\boldsymbol{Y}|\boldsymbol{X_i}]dX_i - (\int \mathbb{E}_{\sim i}[\boldsymbol{Y}|\boldsymbol{X_i}]dX_i)^2 \quad (10)$$

Next, consider the term conditional expectation shown in the equation Eq. (10) which per definition,

$$\mathbb{E}_{\sim i}[\boldsymbol{Y}|\boldsymbol{X_i}] = \int f(X_{\sim i}, X_i)dX_{\sim i} \quad (11)$$

Following the first term of Eq. (10), by taking the square of the above expression and by defining a dummy variable $X'_{\sim i}$, the product of integrals can be written in terms of a multiple integral,

$$\mathbb{E}^2_{\sim i}[\boldsymbol{Y}|\boldsymbol{X_i}] = \int f(X_{\sim i}, X_i)dX_{\sim i} \cdot \int f(X_{\sim i}, X_i)dX_{\sim i} = \iint f(X'_{\sim i}, X_i) \cdot f(X_{\sim i}, X_i)\, dX'_{\sim i}dX_{\sim i} \quad (12)$$

Returning to the definition of variance of conditional expectation Eq. (10),

$$\mathbb{V}_i\left[\mathbb{E}_{\sim i}[\boldsymbol{Y}|\boldsymbol{X_i}]\right] = \iint f(X'_{\sim i}, X_i) \cdot f(X_{\sim i}, X_i)\, dX'_{\sim i}dX - (\int f(X)dX)^2 \quad (13)$$

Finally, the main-effect index can be written as an integral as follow,

$$S_i = \frac{\mathbb{V}_i\left[\mathbb{E}_{\sim i}[\boldsymbol{Y}|\boldsymbol{X_i}]\right]}{\mathbb{V}[\boldsymbol{Y}]} = \frac{\iint f(X'_{\sim i}, X_i)\cdot f(X_{\sim i}, X_i)\, dX'_{\sim i}dX - (\int f(X)dX)^2}{\int f^2(X)dX - (\int f(X)dX)^2} \quad (14)$$

The integral form in Eq. (14) is the basis of Monte Carlo estimation (or the Sobol'-Saltelli method). The same procedure applies for the derivation of the total-effect index (not shown for the sake of brevity).

2.3. Functional Data Analysis (FDA)

Functional data analysis (FDA), a term popularized by [7], refers to the statistical analyses of data that are *functions*. The main assumption of FDA is that the data has sufficient smoothness, defined by the existence of derivatives up to a certain order. The goal of FDA related to this work is to describe the *overall* variation of functions using smaller set of scalars. These scalars can then be used as the QoIs for GSA. FDA used in the present study involves a series of procedures described below.

2.3.1. Functional output and its representation

The assumption of continuity within a discrete dataset (such as numerical code output) is made explicit through a functional representation. Following [7], the recommended representation is through a linear combinations of basis functions. In this paper, the B-spline basis function expansion was used due to its flexibility and its wide availability as an open numerical library. A detailed discussion on B-spline expansion and interpolation can be found in [8].

2.3.2. Curve registration by Landmark

Two types of variations are often simultaneously present in a functional dataset; the variation in magnitude and the variation in phase. The presence of these two types of variation makes even the definition of mean function difficult. To tackle this, both types of variation are first separated through a registration procedure [9]. The procedure transforms the time argument using a *warping* function such that there is less phase variation in the dataset. For the present work, the *landmark* registration type is employed. In a functional dataset with phase variation, this particular type of registration forces important events of a curve (its *landmarks*) to occur at the same time.

2.3.3. Functional principal component analysis (fPCA)

Separation of phase variation from the magnitude variation by registration allows the definition of proper mean function. From there, the notion of functional variation can be defined. The covariance function of a set of curve $\{Y_i(t), i = 1,2, \dots N, t \in [t_a, t_b]\}$ is defined as,

$$v(t_1, t_2) \equiv \frac{1}{N}\sum_{i=1}^{N}(Y_i(t_1) - \bar{Y}(t_1)) \cdot (Y_i(t_2) - \bar{Y}(t_2)) \tag{15}$$

To extract more meaningful information from the covariance function, the function is often projected into lower dimension using an orthogonal decomposition. This projection is done through the functional Principal Component Analysis, fPCA (also known as the Karhunen-Loève transform):

$$v(t_1, t_2) = \sum_{k=1}^{+\infty} \rho_k \cdot \xi_k(t_1) \cdot \xi_k(t_2) \tag{16}$$

Where ρ_k is a series of ordered eigenvalues of decreasing value and ξ_k is the orthogonal eigenfunction (the *functional principal component*, or fPC).

The transformation of the covariance function into pairs of eigenvalues and eigenfunction also allows the original dataset $\{Y(t)\}$ to be represented as a series (Karhunen-Loève expansion, an optimal orthogonal expansion),

$$Y_i(t) = \bar{Y}(t) + \sum_{k=1}^{+\infty} \theta_{ki} \cdot \xi_k(t)\,; \;\; i = 1,2, \dots N \tag{17}$$

With the functional principal component scores θ_{ki} defined by orthogonality condition,

$$\theta_{ki} = \int [Y_i(t) - \bar{Y}(t)] \cdot \xi_k(t) dt \tag{18}$$

The formulations given by Eq. (17) and (18) imply that across realizations in the sample $\{Y(t)\}$, any realization $Y_i(t)$ can be represented using a common mean function and sums of deviations from the mean. The deviation terms consist of a set of common eigenfunctions and a set of fPC scores. As such, it leaves the random character of each realization to the score associated to each component. Put differently, the eigenfunctions gives the mode of variations, while the scores quantify the strength of a particular mode (see [10]). These scores will be used as QoIs in the present sensitivity analysis.

2.4. Implementation

An implementation of the Sobol'-Saltelli method was developed in Python (v3) language. For N number of samples and k number of parameters, the Monte Carlo (MC) procedure follows the suggestion given in [6], [11], [12] (by sampling and resampling approach):

1. Generate two $N \times k$ independent random samples from a uniform distribution of $[0, 1]$

$$A = \begin{pmatrix} a_{11} & \cdots & a_{1k} \\ \vdots & \ddots & \vdots \\ a_{N1} & \cdots & a_{Nk} \end{pmatrix}; B = \begin{pmatrix} b_{11} & \cdots & b_{1k} \\ \vdots & \ddots & \vdots \\ b_{N1} & \cdots & b_{Nk} \end{pmatrix} \tag{19}$$

2. Construct k additional matrices where each matrix is matrix A with the i-th column substituted by the i-th column of matrix B

$$A_B^1 = \begin{pmatrix} b_{11} & a_{12} & \cdots & a_{1k} \\ \vdots & \vdots & \ddots & \vdots \\ b_{N1} & a_{N1} & \cdots & a_{Nk} \end{pmatrix}, A_B^i = \begin{pmatrix} a_{11} & \cdots & b_{1i} & \cdots & a_{1k} \\ \vdots & \cdots & \vdots & \cdots & \vdots \\ a_{N1} & \cdots & b_{Ni} & \cdots & a_{Nk} \end{pmatrix}, \ldots, A_B^k \tag{20}$$

3. Rescale each point in the matrices of samples to the actual values of model parameters according to their actual distributions through iso-probabilistic transformation
4. Execute the model with an input vector that corresponds to each row of A, B, and all the A_B^i
5. Consolidate the outputs from all the model executions (with additional post-processing if required) into vectors and calculate the main-effect and total-effect indices using the selected estimators (explained below)

Two estimators for the main-effect indices are considered for this work. The first is proposed by Saltelli et al. in [13]. As an alternative, a second estimator proposed by Janon et al. [14] is also considered. The latter estimator showed a better efficiency, especially for a large variation around a parameter estimate.

The first term in the nominator of Eq. (14) is the same for both Saltelli et al. and Janon et al. estimators and given by,

$$\iint f(X'_{\sim i}, X_i) \cdot f(X_{\sim i}, X_i)\, dX'_{\sim i} dX \cong \frac{1}{N}\sum_{j=1}^{N} f(B)_j \cdot f\left(A_B^i\right)_j \tag{21}$$

where the subscript *j* corresponds to the row of sample model parameters matrices (Eq. (19)-(20)).

The MC approximations for the second term of the nominator and the denominator differ for the two estimators and they are given in Table I.

Table I. Two Monte Carlo estimators for the terms in the Eq. (14) to calculate the main-effect indices

Estimator	$\mathbb{E}[\boldsymbol{Y}] = \int \boldsymbol{f(X)dX}$	$\mathbb{V}[\boldsymbol{Y}] = \int \boldsymbol{f^2(X)dX} - (\int \boldsymbol{f(X)dX})^{\boldsymbol{2}}$
Saltelli et al. [4]	$\frac{1}{N}\sum_{j=1}^{N} f(A)_j \cdot f(B)_j$	$\frac{1}{N}\sum_{j=1}^{N} f(A)_j^2 - \left(\frac{1}{N}\sum_{j=1}^{N} f(A)_j\right)^2$
Janon et al. [8]	$\frac{1}{N}\sum_{j=1}^{N} \frac{f(B)_j + f\left(A_B^i\right)_j}{2}$	$\frac{1}{N}\sum_{j=1}^{N} \frac{f(B)_j^2 + f\left(A_B^i\right)_j^2}{2} - \left(\frac{1}{N}\sum_{j=1}^{N} \frac{f(B)_j + f\left(A_B^i\right)_j}{2}\right)^2$

To estimate the total-effect indices, the Jansen estimator [15] is recommended in [13]. It reads,

$$\widehat{ST_i} = \frac{\mathbb{E}_{\sim i}[\mathbb{V}_i[Y|X_{\sim i}]]}{\mathbb{V}[Y]} \cong \frac{\frac{1}{2N}\sum_{j=1}^{N}\left(f(A)_j - f\left(A_B^i\right)\right)^2}{\mathbb{V}[Y]} \tag{22}$$

With $\mathbb{V}[Y]$ estimated by the Saltelli et al. estimator given in Table I.

As it can be inferred, the computational cost associated with the computation of all the main-effect and total-effect indices is $N \times (k+2)$ code runs, where N is the number of samples and k is the number of parameters. As comparison, the cost for the Morris method to compute the statistics of the elementary effects is $n_r \times (k+1)$, where n_r is the number of trajectories. However, note that the typical number of Morris trajectories is $< 10^2$, while the number of Sobol' samples amount to $10^3 - 10^4$.

Finally, functional data analysis for code output from a reflood simulation was previously demonstrated in [16]. Here, the methodology is adopted once again and coupled with the set of functional code output from the Sobol'-Saltelli samples. All the computation related to functional data analysis was done in the R−statistical computing environment [17] using the "`fda`" package [18].

3. CASE STUDY: TRACE MODEL OF THE FEBA FACILITY

3.1. The FEBA Facility and the TRACE Model

A series of FEBA (Flooding Experiment with Blocked Arrays) experiments were conducted in the 1980's at the Karlsruhe Institute of Technology to improve knowledge of heat transfer mechanism during reflooding taking into account the effect of flow blockage and spacer grid, as well as to validate the thermal-hydraulics model and codes available then. The facility consisted mainly of a full height 5-by-5 bundle of PWR fuel rod simulators enclosed in stainless steel housing. An approximate cosine power profile was imposed using electrical heater with nominal power of 120% ANS decay heat. The facility and test data are publicly available at the KIT library website (see [19] for details).

The FEBA experiment corresponds to the first test series (with all 7 spacer grids mounted and without blockage) was modeled using several basic components as shown in Figure 1 in a version of TRACE v5.0p3 code (a custom version with several model parameters externalized).

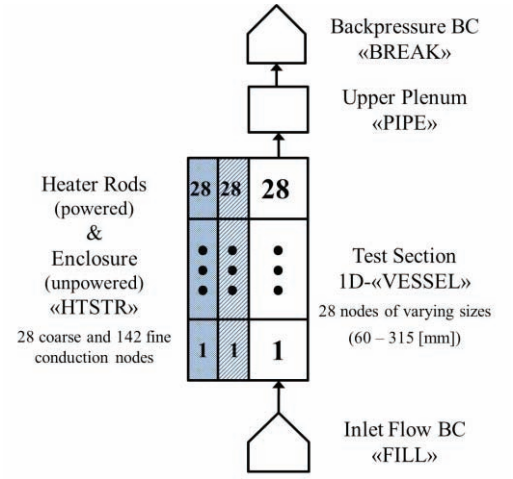

Figure 1. FEBA model in TRACE

3.2. Selected Model Parameters

Variations in the values of the model parameters are modeled as random variables equipped by their probability density function. The choice of the distribution is influenced both by the available information and the purpose of the analysis. As the main aim of present work is to carry out sensitivity analysis, a simple reasonable range of parameters variations are assumed. Note that the present work is not aimed at uncertainty quantification as the selected parameter variations were not established as *uncertainty*.

For a given sampled model parameter, one of three modes of perturbation possible: additive, substitutive, and multiplicative. In additive mode, the sampled parameter value is added to the nominal values. In substitutive mode, the sampled parameter directly substitutes the nominal value. And in multiplicative mode, the nominal value is multiplied with the sampled value.

As shown in Table II, the parameter list involves perturbing various parameters related to:

1. Thermal-hydraulics boundary conditions (parameters 1 to 4)
2. Material properties (parameter 5 to 13)
3. Spacer grid model, including models for the pressure loss and convective heat transfer coefficient enhancement (parameter 14 and 15)

4. TRACE constitutive models relevant to reflood simulation (parameter 16 to 25). In TRACE, reflood phenomena was modelled using the post-CHF heat – hydrodynamic transfer package. This particular package consists of two distinct flow regimes: the Inverted Annular Film Boiling (IAFB) and the Dispersed Film Flow Boiling (DFFB). Details on the models can be found in [20]
5. Quench temperature as calculated by TRACE (parameter 26)

Table II. Selected TRACE model parameters and their range of variations

No	Parameter ID	Description	Distribution	Range of Variation	Nominal Value	Mode of Perturbation	Unit
1	break_ptb	Outlet Pressure	Uniform	[0.90, 1.10]	1.0	Multiplicative	[-]
2	fill_tltb	Inlet Water Temp.	Uniform	[-5.00, +5.00]	0.0	Additive	[K]
3	fill_vmtbm	Inlet Water Velocity	Uniform	[0.90, 1.10]	1.0	Multiplicative	[-]
4	power_rpwtbr	Heater Rods Power	Uniform	[0.95, 1.05]	1.0	Multiplicative	[-]
5	nic_cond	Conductivity (Nichrome)	Uniform	[0.95, 1.05]	1.0	Multiplicative	[-]
6	nic_cp	Specific Heat (Nichrome)	Uniform	[0.95, 1.05]	1.0	Multiplicative	[-]
7	nic_emis	Emissivity (Nichrome)	Uniform	[0.90, 1.00]	0.95	Multiplicative	[-]
8	mgo_cond	Conductivity (Magnesium Oxide)	Uniform	[0.8, 1.2]	1.0	Multiplicative	[-]
9	mgo_cp	Specific Heat (Magnesium Oxide)	Uniform	[0.8, 1.2]	1.0	Multiplicative	[-]
10	vessel_epsw	Wall Roughness	Uniform	[6.1E-7, 2.44E-6]	1.5E-6	Substitutive	[m]
11	ss_cond	Conductivity (Stainless Steel)	Uniform	[0.95, 1.05]	1.0	Multiplicative	[-]
12	ss_cp	Specific Heat (Stainless Steel)	Uniform	[0.95, 1.05]	1.0	Multiplicative	[-]
13	ss_emis	Emissivity (Stainless Steel)	Uniform	[0.56, 0.94]	0.84	Multiplicative	[-]
14	kGridSV	Spacer Grid ΔP	Uniform	[0.25, 1.75]	1.0	Multiplicative	[-]
15	gridHTEnh	Spacer Grid HTC Enhancement	Log-uniform	[0.50, 2.00]	1.0	Multiplicative	[-]
16	iafbWallHTC	Wall HTC (IAFB)	Log-uniform	[0.50, 2.00]	1.0	Multiplicative	[-]
17	dffbWallHTC	Wall HTC (DFFB)	Log-uniform	[0.50, 2.00]	1.0	Multiplicative	[-]
18	iafbLIHTC	Liquid-Interface HTC (IAFB)	Log-uniform	[0.25, 4.00]	1.0	Multiplicative	[-]
19	iafbVIHTC	Vapor-Interface HTC (IAFB)	Log-uniform	[0.25, 4.00]	1.0	Multiplicative	[-]
20	dffbLIHTC	Liquid-Interface HTC (DFFB)	Log-uniform	[0.25, 4.00]	1.0	Multiplicative	[-]
21	dffbVIHTC	Vapor-Interface HTC (DFFB)	Log-uniform	[0.25, 4.00]	1.0	Multiplicative	[-]
22	iafbIntDrag	Interfacial Drag (IAFB)	Log-uniform	[0.25, 4.00]	1.0	Multiplicative	[-]
23	dffbIntDrag	Interfacial Drag (DFFB)	Log-uniform	[0.25, 4.00]	1.0	Multiplicative	[-]
24	iafbWallDrag	Wall Drag (IAFB)	Log-uniform	[0.50, 2.00]	1.0	Multiplicative	[-]
25	dffbWallDrag	Wall Drag (DFFB)	Log-uniform	[0.50, 2.00]	1.0	Multiplicative	[-]
26	tempQuench	Quenching Temp.	Uniform	[-50.0, +50.0]	TRACE*	Additive	[K]

3.3. Simulation Experiments

The global sensitivity methodology described in Section 2 is applied to analyze the FEBA experiment model in TRACE. Only FEBA Test No. 216 (with inlet velocity of 3.8E-2 [m.s-1] and system pressure of 4.1 [bar]) was considered. Only the cladding temperature evolution only at the middle of the assembly (1.625 [m]) was considered in this work. The duration of the transient is 600 [s]. Fig. 2 illustrates the

* As calculated internally by TRACE code

variation of the TRACE output (rod temperature evolution at mid-assembly) due to variation in the model parameters given in Table II. Shown in the figure are outputs from 100 randomly sampled combinations of the model parameters. Each run of requires approximately 600 [CPU.s].

The experiment was carried out in two parts. The first part is aimed to screen out any possible non-influential parameters using the Morris method. The application of the Morris method on the TRACE model of FEBA facility to rank parameter importance was previously demonstrated in [21]. As the number of parameters is directly proportional to the number of code runs, a screening procedure allows larger samples for less number of code runs resulting in more precise Monte Carlo estimates. For the sake of comparison, the Sobol'-Saltelli method was also employed to obtain parameter importance ranking. All the Sobol' samples used in this study were generated using a Sobol' quasi-random sequence generator given by [22]. The second part of the experiment deals with detailed sensitivity analysis.

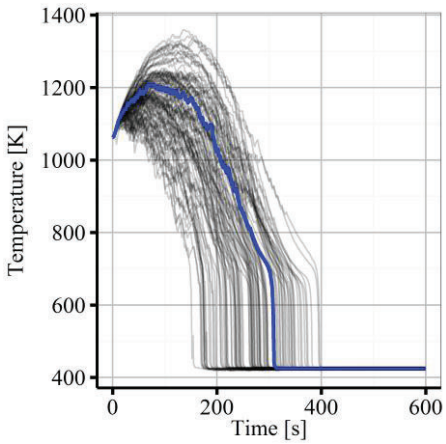

Figure 2. Variation of temperature evolution from 100 TRACE outputs due to variation in parameters given in Table II. Blue line is the reference run (a run with nominal parameter values).

The analysis of the transient output using FDA technique to extract the functional principal component scores for each realization was done after all the samples were generated. All the steps of FDA (B-spline representation, registration, and functional principal component analysis) were previously demonstrated in the context of reflood simulation output [16]. The resulting principal component scores for each Sobol' samples were then fed back to the Python routine to compute the sensitivity indices. Finally, to give a measure of the uncertainty in all of the indices estimated by the Monte Carlo procedure, a standard error and 95% percentile confidence interval were constructed using bootstrap technique [23].

4. RESULTS AND DISCUSSION

4.1. Screening Analysis

A screening analysis to identify any non-influential parameter using the Morris screening method was first carried out. Previous study showed that 40 Morris trajectories were sufficient to obtain stable importance ranking for the same model [21]. The average temperature at the mid height of the assembly (defined as the integral over the transient divided by the duration) was chosen as the QoI in the analysis as it is able to capture the overall change of temperature during the transient as a single number.

For comparison purpose, the Sobol'-Saltelli method was also carried out on the model using 1,000 samples. The results are given in Table III. For the Sobol'-Saltelli method, the estimated indices are equipped with their 95% bootstrapped confidence interval. Though the intervals are at times can be large, the results are consistent with the Morris method, especially in the top ten ranks. A more important

finding is the non-influential parameters as indicated by the total-effect indices with a very high certainty. The 16 non-influential parameters are deemed appropriate to be excluded from further analysis.

Table III. Comparison of parameter importance ranking using the Morris screening method and Sobol'-Saltelli method (n_r is the number of Morris trajectories, while N is the number of Sobol' samples). Entries in bold are the important model parameters to be considered in further analysis.

No.	Parameter	Morris Screening (n_r = 40; 1,080 runs)			Sobol'-Saltelli (N = 1,000; 28,000 runs)		
		Rank	μ^*	σ	Rank	$\widehat{S}_i$	$\widehat{ST}_i$
1	break_ptb	**10**	0.11	0.09	**9**	0.01 (-0.08, 0.11)	0.02 (0.01, 0.02)
2	fill_tltb	14	0.03	0.02	13	0.00 (-0.02, 0.02)	0.00 (0.00, 0.00)
3	fill_vmtbm	**6**	0.21	0.06	**5**	0.04 (-0.12, 0.20)	0.04 (0.04, 0.05)
4	power_rpwtbr	**9**	0.12	0.07	**10**	0.00 (-0.10, 0.09)	0.02 (0.01, 0.02)
5	nic_cond	26	0.00	0.01	24	-0.01 (-0.01, 0.00)	0.00 (0.00, 0.00)
6	nic_cp	12	0.04	0.02	15	-0.02 (-0.05, 0.02)	0.00 (0.00, 0.00)
7	nic_emis	21	0.01	0.01	25	-0.01 (-0.02, 0.00)	0.00 (0.00, 0.00)
8	mgo_cond	20	0.01	0.01	19	-0.00 (-0.01, 0.01)	0.00 (0.00, 0.00)
9	mgo_cp	11	0.06	0.04	11	-0.02 (-0.07, 0.04)	0.01 (0.01, 0.01)
10	vessel_epsw	24	0.01	0.01	21	0.00 (-0.01, 0.01)	0.00 (0.00, 0.00)
11	ss_cond	22	0.01	0.01	17	0.00 (-0.01, 0.01)	0.00 (0.00, 0.00)
12	ss_cp	15	0.02	0.03	14	-0.01 (-0.03, 0.02)	0.00 (0.00, 0.00)
13	ss_emis	17	0.01	0.02	26	-0.01 (-0.03, -0.00)	0.00 (0.00, 0.00)
14	kGridSV	13	0.04	0.02	12	-0.01 (-0.04, 0.03)	0.00 (0.00, 0.00)
15	gridHTEnh	**1**	0.56	0.25	**1**	0.35 (-0.10, 0.83)	0.39 (0.35, 0.44)
16	iafbWallHTC	**7**	0.15	0.09	**7**	0.01 (-0.12, 0.14)	0.03 (0.03, 0.04)
17	dffbWallHTC	**3**	0.43	0.22	**2**	0.21 (-0.16, 0.60)	0.23 (0.21, 0.26)
18	iafbLIHTC	19	0.01	0.01	23	-0.01 (-0.02, 0.00)	0.00 (0.00, 0.00)
19	iafbVIHTC	16	0.01	0.02	18	-0.01 (-0.02, 0.01)	0.00 (0.00, 0.00)
20	dffbLIHTC	25	0.01	0.01	20	0.00 (-0.01, 0.01)	0.00 (0.00, 0.00)
21	dffbVIHTC	**4**	0.32	0.15	**4**	0.08 (-0.13, 0.30)	0.08 (0.07, 0.09)
22	iafbIntDrag	**5**	0.21	0.25	**8**	0.01 (-0.12, 0.15)	0.03 (0.03, 0.03)
23	dffbIntDrag	**2**	0.53	0.30	**3**	0.18 (-0.16, 0.53)	0.20 (0.18, 0.22)
24	iafbWallDrag	23	0.01	0.01	22	0.00 (-0.01, 0.01)	0.00 (0.00, 0.00)
25	dffbWallDrag	18	0.01	0.01	16	0.00 (-0.01, 0.01)	0.00 (0.00, 0.00)
26	tempQuench	**8**	0.13	0.06	**6**	0.03 (-0.10, 0.17)	0.03 (0.03, 0.04)

To check the consistency of the screening, The distribution of the outputs of the full model (26 inputs) versus the screened-parameter model (10 inputs) are compared in Table IV. Both distributions were obtained with 1,000 Sobol' samples. From the table, the statistics for both models are comparable especially with respect to the dispersion measures. As the two yields similar distributions, this further supports the fact that the screened-out parameters are indeed non-influential with respect to the output.

Table IV. Comparison between two TRACE output statistics of the full model (26 inputs) and the screened model (10 inputs) both using 1,000 Sobol samples.

Sample Statistics	$T_{\max}$			$\overline{T}_{\text{integrated}}$		
	Full Model	Screened Model	Unit	Full Model	Screened Model	Unit
Mean	1,196.5	1,196.2	[K]	768.5	764.8	[K]
Median	1,190.4	1,189.4	[K]	761.0	761.6	[K]
1st Quartile	1,149.3	1,150.0	[K]	702.0	696.3	[K]
3rd Quartile	1,235.9	1,233.9	[K]	828.3	827.0	[K]
Interquartile Range	86.6	83.9	[K]	126.3	131.0	[K]
Standard Deviation	58.9	58.7	[K]	88.9	91.5	[K]
Coefficient of Variation	0.049	0.049	[-]	0.116	0.120	[-]

4.2. Convergence of the Sobol Indices

The convergence of the Sobol' indices using a given estimator can be investigated from their evolutions with the increasing number of samples. Shown in Fig. 3 is the evolution of main-effect indices with maximum temperature as the QoI. It can be seen that the Saltelli et al. estimator performs poorly.

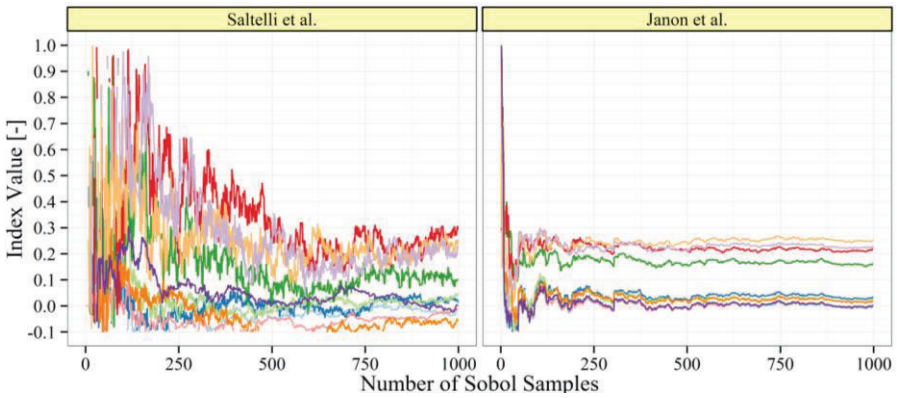

Figure 3. Evolution of main-effect sensitivity indices using two different estimators (Saltelli et al. and Janon et al.) as a function of number of samples with maximum temperature as the QoI.

If the main purpose of the sensitivity analysis is simply to rank parameter importance with respect to the QoI then from both figures, it can be concluded that Janon et al. estimator requires fewer sample. However, the stabilization of the estimator shown is not sufficient to establish a robust quantitative estimate of the indices as Monte Carlo (MC) estimation entails sampling uncertainty due to the finite number of samples. Such an uncertainty need to be assessed and then reported for all the index estimates.

In this paper, an empirical convergence study was established using 3 different numbers of samples (250; 500; 1,000) and for each the 95% confidence interval length was calculated using bootstrap technique (with 10,000 replicas). The results are shown Fig. 4 for the maximum temperature as the QoI. Evidently, with respect to the maximum temperature, the Janon et al. estimator is the more efficient estimator. The uncertainty of the Saltelli et al. estimator is high for numbers of samples in the range of thousands. Also, the efficiency of the Saltelli et al. estimator is also found to be more sensitive to the choice of estimands.

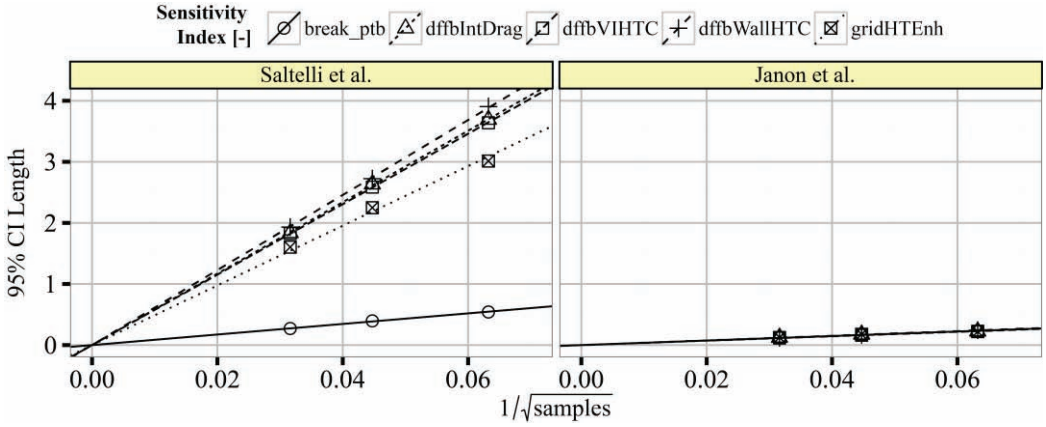

Figure 4. The 95% percentile bootstrapped confidence interval (CI) length as function of the number of samples for 5 estimated Sobol' indices with respect to the maximum temperature using two different estimators. The lines shown are the *regression through the origin* (RTO) lines.

However, further investigation also revealed that efficiency of an estimator depended on the estimand. In Figure 5, the first principal component score (See Section 2.3) was taken as the QoI and both estimators was found to be comparable, with the Saltelli et al. estimator being slightly more efficient.

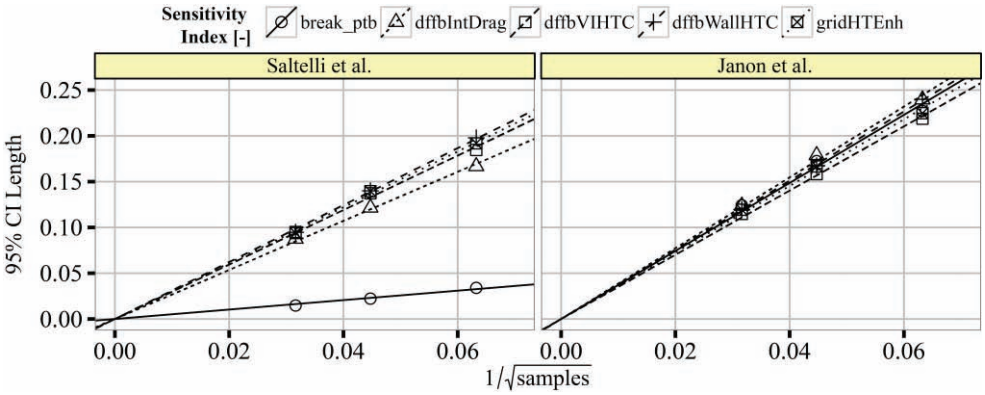

Figure 5. The 95% percentile bootstrapped confidence interval (CI) length as function of number of samples for 5 estimated Sobol' indices with respect to the first functional principal component (fPC1) scores.

The plots such as that shown in Figure 4 and Figure 5 can be useful in the planning of the simulation experiment. As can be inferred from the two figures, confidence interval of a given estimator depends on the estimand, the estimator used, and the number of samples. The regression lines also indicate the projection of reduction in confidence interval length. Though not shown here, the results for total-effect indices using the Jansen's estimator were found to have good efficiency, reaching below 10% CI length for 1,000 samples across all QoIs. Benefitting from the screening procedure (10 instead of 26 inputs) and by looking at the empirical convergence, a total of 2,000 samples (which corresponds to 22,000 TRACE runs) were generated for more detailed sensitivity analyses discussed below.

4.3. Sobol' Indices for the Physical Output

Two relevant QoIs for a reflood simulation are the maximum temperature and the time of quenching. As shown in Fig. 6, the variation of the maximum temperature (with standard deviation of 60 [K]) was driven mainly by four model parameters (contributing over 84% of the variation). One was related to the grid heat transfer (HT) enhancement model (18%) and the others were related to the DFFB regime model (up to 66% combined). Moreover, as the sum of the main-effect indices was close to 1, it can be concluded that the parameters were not interacting with respect to this QoI (See Eq. (7))

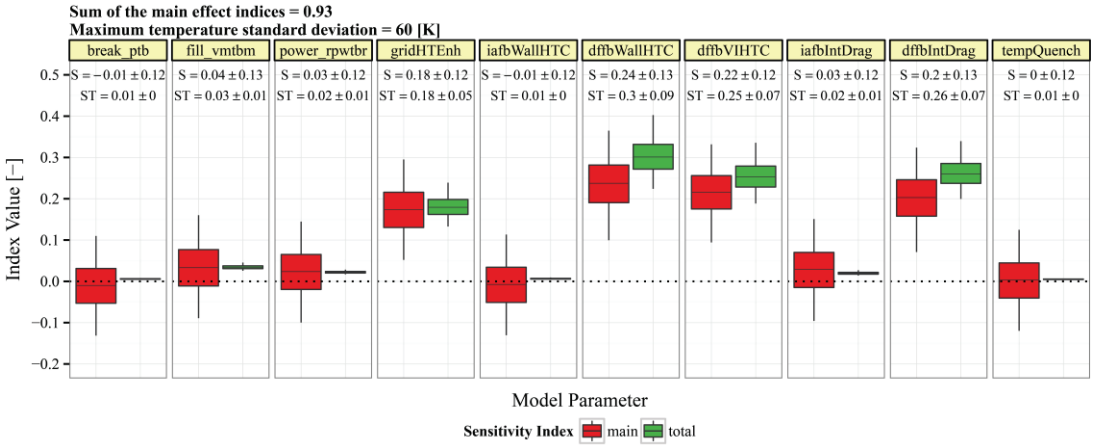

Figure 6. Sensitivity indices, main- and total-effect, with maximum temperature as the QoI.

The sensitivity with respect to the quenching time painted a different picture (Fig. 7). The variation of the quenching time (standard deviation of 60.8 [s]) was driven mainly by spacer grid HT enhancement (with over 50% variance contribution). The DFFB -related parameters are next in line with around 20% contribution. Similar to the case of maximum temperature, no strong interaction-effects were observed.

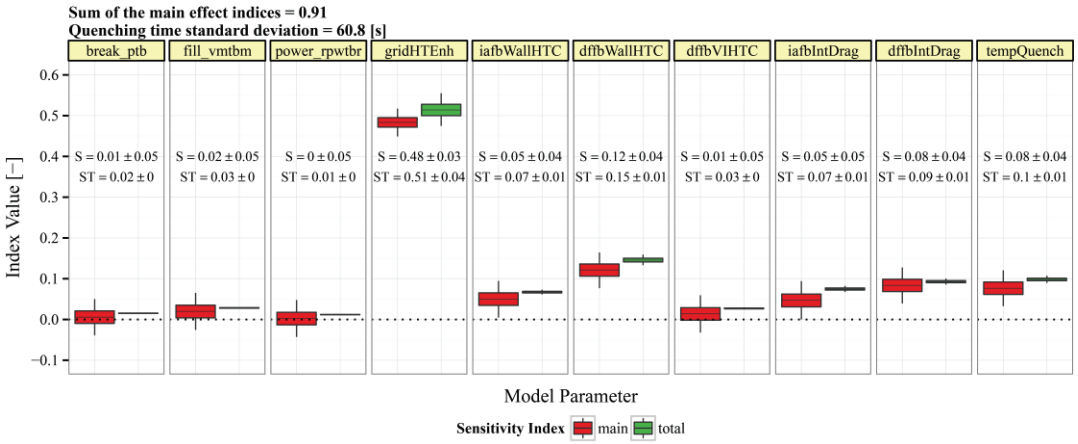

Figure 7. Sensitivity indices, main- and total-effect, with quenching time as the QoI.

The use of scalar function such as the maximum, or by referring to a particular event (quenching) as the QoI were important and intuitive as it corresponded directly to a variation of physical quantities. Now, the temperature at each time step is taken as the QoI and the sensitivity indices are calculated at each time step. Shown in Fig. 8 and in Fig. 9 are the evolution of main-effect (Eq. (8)) and interaction-effect (Difference between Eq. (9) and Eq. (8)) indices, respectively. They correspond to the reflood temperature transient in which the phase variations between realizations were removed by registration.

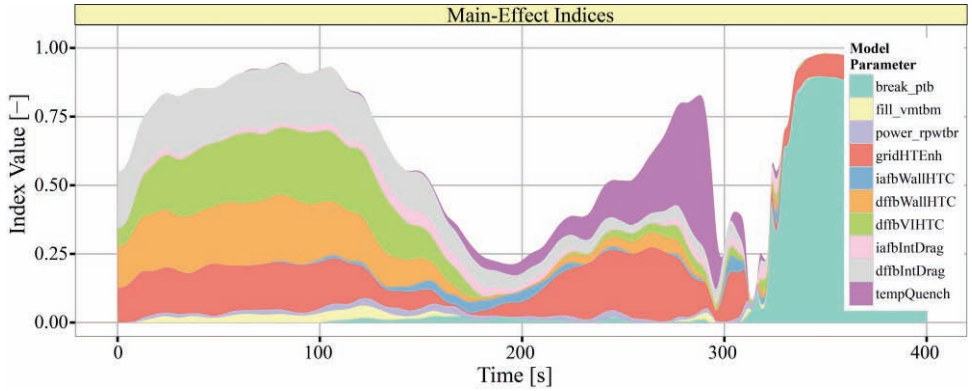

Figure 8. Stacked area chart depicting the evolution of the main-effect sensitivity indices with the registered mid-assembly temperature as the QoI.

Both figures show that the parameters relative importance and their interactions in the dynamic model are highly time-dependent. With respect to the temperature, up to 120 [s] the model parameters were non-interacting as all the main-effect indices almost summed up to 1.0. The grid HT and the DFFB models were found to be the most important in this time range. But, from 120 [s] onward, stronger interactions takes place and the main-effect indices could not explain for more than 20% of the temperature variance. The quench temperature which for the most part of transient was non-influential tops after 200 [s]. Around 300 [s] the temperature transient variations suddenly were driven only by parameters interactions (Fig. 9). Finally, the variation of the pressure boundary explained the temperature variance in equilibrium.

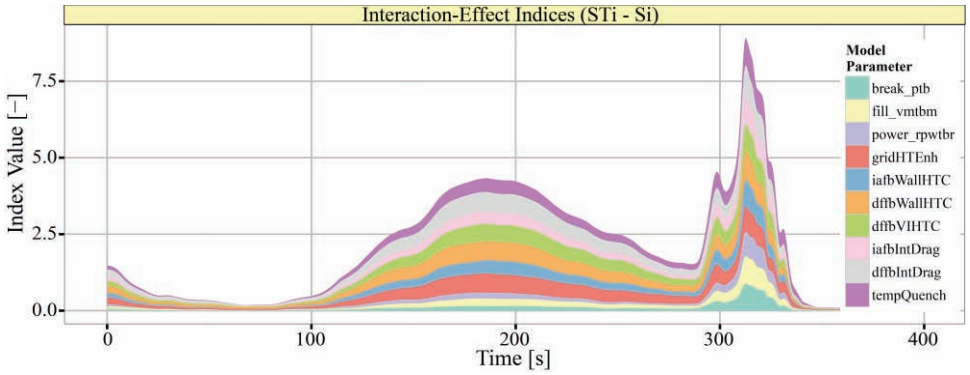

Figure 9. Stacked area chart depicting the evolution of the interaction-effect sensitivity indices with the registered mid-assembly temperature as the QoI.

The two plots above are useful to give the general picture of how the model behaves during the transient, yet they give an incomplete picture in terms of how a parameter actually influences the transient. Besides, no indication of the magnitude of output variation is given by the plots. The temperature variation in the first 100 [s] of the transient amounts to 60 [K] in standard deviation while the last part of the transient (where the pressure boundary becomes very important) amounts only to 2 [K].

4.4. Sobol' Indices for the Functional Principal Component

To complement the previous results, sensitivity analysis was also carried out on the functional principal component (fPC) scores of the overall output of reflood transient. The use of functional principal components can further clarify some questions regarding the form (or shape) of variation in certain period of time implied by looking at the evolution of the indices. The fPC analysis was carried out on all the Sobol' samples and resulted in three main principal components accounting for 90% of the functional variation of the reflood transient. Presented here are the first two components (accounting 87% variation).

The 1st functional principal component (the eigenfunction) of the reflood transient and the effect of its perturbation around the mean reflood transient function are shown in Fig. 10. The perturbation is done by adding and subtracting the mean function by the eigenfunction multiplied by twice the standard deviation of the associated scores. This eigenfunction corresponds to a mode of variation which can be interpreted as the variation in vertical shift of the temperature transient prior to quenching (temperature ramp). It is the strongest mode of variation, accounting for 55% of the overall transient variation.

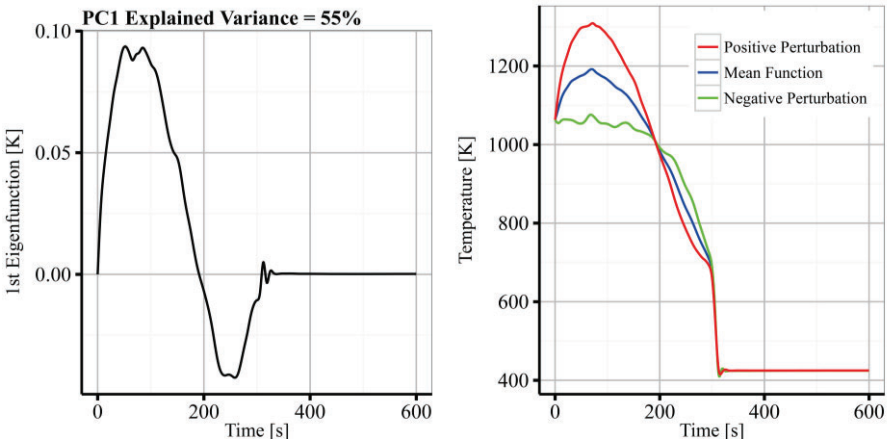

Figure 10. The 1st functional principal components and the effect of its perturbation on the mean function.

The Sobol' indices for this particular mode of variation are given in Fig. 11. Evidently, the variation of the temperature vertical shift was due to the spacer grid HT enhancement and the DFFB flow regime-related model parameters. The other parameters are almost non-influential with high certainty. This result is consistent with the results of max. temperature as it represents the variation on this part of transient.

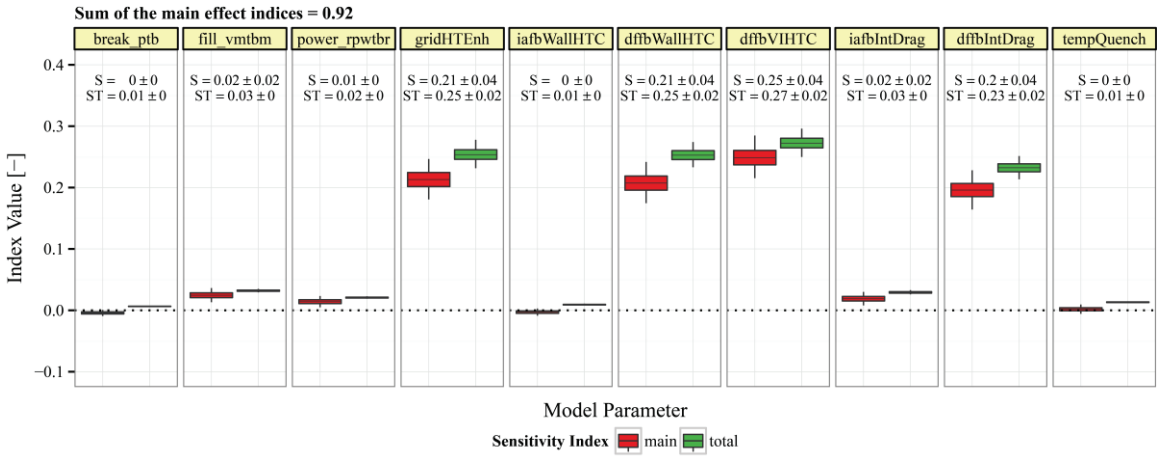

Figure 11. Sensitivity indices with respect to the 1st functional principal components. The boxplots show the bootstrap samples of each estimate, while the estimates and their $1.96 \times$ Standard Error are written inside.

Fig. 12 shows the 2nd fPC of the reflood transient and the effect of its perturbation on to the mean function. This mode of variation can be interpreted as the variation in the temperature descent after reaching the maximum prior to quenching. Visibly, some realizations tend to have more convexity in the temperature descent than the others. It constitutes about 32% of the overall functional variation.

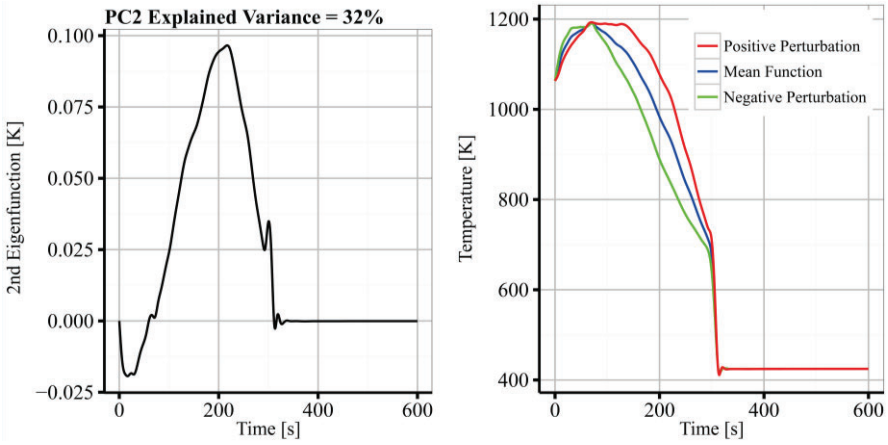

Figure 12. The 2nd functional principal components and the effect of its perturbation on the mean function.

As before, Fig. 13 below gives the sensitivity indices for this particular mode of variation. Contrary to the previous mode of variation, the variation of the 2nd fPC can only be explained through interactions between parameters. All the main-effect indices summed up only to 32% while all the reflood specific model parameters are highly interacting. The differences between main- and total-effect are the largest for DFFB-related parameters.

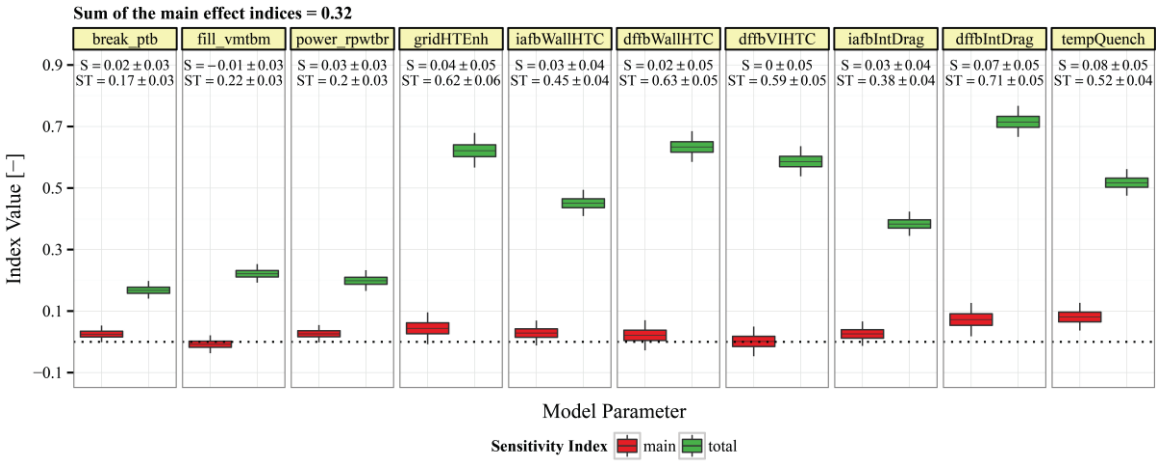

Figure 13. Sensitivity indices with respect to the 2nd functional principal components. The boxplots show the bootstrap samples of each estimate, while the estimates and their $1.96 \times$ Standard Error are written inside.

4.5. Discussion

In the present work, the method of Morris was used as a screening tool to filter out non-influential parameters from further analysis. It was shown that such reduction was valuable in the downstream analyses. Yet, as it was observed in [21] the method can be used to derive sensitivity measure in its own right albeit a qualitative one (referring to the results in the Table III for the Morris method, μ^* and σ are sensitivity measures). They are deemed qualitative as they do not quantify the contribution of the parameters variations to the output variation. Besides, the method does not distinguish between parameters interaction and nonlinearities. On the contrary, the quantitative Sobol'-Saltelli method overcomes these problems by giving more precise definition of the sensitivity measure (defined in term of proportion of output variance) as well as more precise term of parameters interactions.

The results presented above showed the consistency of the phenomenological model implemented in TRACE in simulating an experimental reflood transient. The experimental boundary conditions of the test case (FEBA test No. 216) refer to a low bottom flooding rate and according to the phenomenological model, the Dispersed Film Flow Boiling Regime dominates the heat transfer [20]. This is confirmed when looking at the sensitive parameters with respect to the cladding temperature transient. However, it is shown here for the first time how the variations of the important parameters impact the model output and by how much. The transient output of reflood simulation complicates the characterization of variation in functional sense, beyond conventional scalar output (the maximum temperature and the quenching time)

Different aspects of transient output variations were exposed using functional principal components analysis (fPCA). fPCA is a data-driven approach that extracts the important features from the data itself. It gives a more complete picture on how certain parameter affect certain aspect of model behavior. As it was shown, the model parameters influence the temperature ramp of the reflood transient with minor interactions among themselves. In other words, the model is additive and likely also to be identifiable with respect to temperature data. The parameters can either be informed by the available data or the output variance can be reduced by reducing the variance in the input parameters.

On the other hand, the temperature descent up to and at quenching were influenced by interactions between parameters. This might be explained by the fact that the temperature descent involves flow regime changes and the conditions leading to the changes depend strongly on simultaneous perturbation of the parameters. The high level of parameters interactions gives an indication that the model is non-identifiable with respect to the temperature response at that particular part of the transient.

Finally, a remark should be given on the nature of variations of the model parameters used in the present study (as given in Table II). As was warned in [24], the results of sampling-based sensitivity analysis depends on the distributions assigned to the parameters; as such the distributions have to be assigned properly to avoid spurious results. The spurious results or conclusions from the sensitivity study can be avoided by making explicit the purpose of the analysis. Indeed, the choice between distributions is guided by the available data as well as the purpose of the analysis. In Table II, the variations of material properties and of the boundary conditions were derived from material properties database and the experimental facility specification, respectively.

However, the ranges of variation of the model parameters (parameters no. 14 to 26 in Table II) are chosen based on the aim of the present work: to investigate which the model parameters the output or model behavior are sensitive to. Added to the lack of experimental values for these parameters, uniform and log-uniform with reasonably large bounds are convenient forms to model the variations in those parameters. Specifically, it is of interest to investigate how large parameter perturbations affect the model output. The choice of distribution adopted here might not be as rigorous as was prescribed in [24] especially for the purpose of uncertainty quantification, but nevertheless the results of the analysis can still be useful as long as the aim of the analysis is made clear and any interpretation of the results is made within the framework sof the chosen distributions.

5. CONCLUSION

A methodology for global sensitivity analysis of transient code output has been presented in this paper. The goal was to carry out global sensitivity analysis, taking into account any presence of parameters interactions, on a transient simulation. The particular objectives of the sensitivity analysis are to identify the most important parameters contributing to the output variation and to expose complex parameters interaction in a time-dependent simulation. Additional set of quantities of interest (QoI) was derived using functional data analysis (FDA) techniques to characterize the overall functional output variation.

The methodology was applied to a reflood simulation at the FEBA facility using TRACE code. The value of parameter screening using the inexpensive Morris method (supported by the results of Sobol`-Saltelli method) was demonstrated. The non-influential parameters were then excluded from a detailed variance decomposition using larger number of samples. The method was successful in apportioning the variation of scalar physical outputs, maximum temperature and time of quenching in terms of the variation of the input parameters. The results are consistent with previously published results, and have been made more precise using Sobol' indices (proportion of output variances due to input variances) complemented with their uncertainties due to Monte Carlo estimation procedure.

However, when considering the whole temperature transient by using QoIs based on FDA, it was found that parameters importance and the nature of their interactions changed during transient. During the early phase of the transient during when the temperature is increasing and during the early reflooding phase, the simulation model showed weak interactions among the prominent model parameters (Grid HT enhancement model as well as the parameters related to DFFB regime). But, during the temperature descent and around quenching, most of the variation in the cladding temperature evolution could only be attributed to parameters interactions. This demonstrates the added-value of the newly derived QoIs for sensitivity analysis of transient simulation models, in complementing the more conventional QoIs based on extreme output values such as the maximum temperature and the quenching time.

ACKNOWLEDGMENTS

This work was partly funded by the Swiss Federal Safety Inspectorate (ENSI) and the Swiss Federal Office for Energy (BFE). The authors thank s Dr. Gregory Perret of the LRS, Paul Scherrer Institut for his comments on this work.

REFERENCES

1. M. D. Morris, "Factorial Sampling Plans for Preliminary Computational Experiments," *Technometrics*, **33**(2), pp. 161–174 (1991).
2. F. Campolongo, J. Cariboni, and A. Saltelli, "An effective screening design for sensitivity analysis of large models," *Environ. Model. Softw.*, **22**(10), pp. 1509–1518 (2007).
3. G. Li, C. Rosenthal, and H. Rabitz, "High Dimensional Model Representations," *J. Phys. Chem. A*, **105(**33), pp. 7765–7777 (2001).
4. H. Rabitz, Ö. F. Aliş, J. Shorter, and K. Shim, "Efficient input—output model representations," *Comput. Phys. Commun.*, **117(**1), pp. 11–20 (1999).
5. I. M. Sobol′, "Global sensitivity indices for nonlinear mathematical models and their Monte Carlo estimates," *Math. Comput. Simul.*, **55**, pp. 271–280 (2001).
6. T. Homma and A. Saltelli, "Importance measures in global sensitivity analysis of nonlinear models," *Reliab. Eng. Syst. Saf.*, **52(**1), pp. 1–17 (1996).
7. J. O. Ramsay and B. W. Silverman, *Functional data analysis*. New York: Springer (2005).
8. P. H. Eilers and B. D. Marx, "Flexible smoothing with B-splines and penalties," *Stat. Sci.*, **11(**2), pp. 89–102 (1996).
9. Ramsay, James O. and X. Li, "Curve Registration," *J. R. Stat. Soc. Ser. B Stat. Methodol.*, **60(**2), pp. 351–363 (2002).
10. C. Maccone, "A simple introduction to the KLT (Karhunen—Loève Transform)," in *Deep Space Flight and Communications*, Germany: Springer, 2009, pp. 154–179.
11. D. Wicaksono, O. Zerkak, and A. Pautz, "Sensitivity Analysis of a Bottom Reflood Simulation using the Morris Screening Method," in *The 10th International Topical Meeting on Nuclear Thermal-Hydraulics, Operation and Safety (NUTHOS-10)*, Okinawa, Japan (2014).
12. G. E. B. Archer, A. Saltelli, and I. M. Sobol, "Sensitivity measures,anova-like Techniques and the use of bootstrap," *J. Stat. Comput. Simul.*, **58**(2), pp. 99–120 (1997).
13. A. Saltelli, "Making best use of model evaluations to compute sensitivity indices," *Comput. Phys. Commun.*, **145**(2), pp. 280–297 (2002).
14. A. Saltelli, P. Annoni, I. Azzini, F. Campolongo, M. Ratto, and S. Tarantola, "Variance-based sensitivity analysis of model output. Design and estimator for the total sensitivity index," *Comput. Phys. Commun.*,**181(**2), pp. 259–270 (2010).
15. A. Janon, T. Klein, A. Lagnoux, M. Nodet, and C. Prieur, "Asymptotic normality and efficiency of two Sobol index estimators," *ESAIM Probab. Stat.*, **18**, pp. 342–364 (2014).
16. M. J. W. Jansen, "Analysis of variance designs for model output," *Comput. Phys. Commun.*, **117**, pp. 35–43 (1999).
17. D. Wicaksono, O. Zerkak, and A. Pautz, "Exploring Variability in Reflood Simulation Results: An Application of Functional Data Analysis," in *The 10th International Topical Meeting on Nuclear Thermal-Hydraulics, Operation and Safety (NUTHOS-10)*, Okinawa, Japan (2014).
18. R Core Team, *R: A Language and Environment for Statistical Computing*. Vienna, Austria: R Foundation for Statistical Computing (2014).
19. J. O. Ramsay, H. Wickham, S. Graves, and G. Hooker, *fda: Functional Data Analysis, R Package*. (2014).
20. P. Ihle and K. Rust, *FEBA-Flooding Experiments with Blocked Arrays: Evaluation Report*. Kernforschungszentrum Karlsruhe (1984).
21. US NRC, "TRACE V5.0p3 Theory Manual," United States Nuclear Regulatory Commission (U.S NRC), Washington, DC (2012).
22. S. Joe and F. Y. Kuo, "Constructing Sobol Sequences with Better Two-Dimensional Projections," *SIAM J. Sci. Comput.*, **30(**5), pp. 2635–2654 (2008).
23. B. Efron and R. Tibshirani, "Bootstrap Methods for Standard Errors, Confidence Intervals, and Other Measures of Statistical Accuracy," *Stat. Sci.*, **1(**1), pp. 54–77 (1986).
24. M. Ionescu-Bujor and D. G. Cacuci, "A Comparative Review of Sensitivity and Uncertainty Analysis of Large-Scale Systems - II: Statistical Methods," *Nucl. Sci. Eng.*, **147**, pp. 204–217 (2004).